ETSU Faculty Works | Faculty Works

8-15-2009

Gene Expression Analyses of Neurons, Astrocytes, and Oligodendrocytes Isolated by Laser Capture Microdissection From Human Brain: Detrimental Effects of Laboratory Humidity

Gregory A. Ordway
East Tennessee State University, ordway@etsu.edu

Attila Szebeni
East Tennessee State University

Michelle M. Duffourc
East Tennessee State University, duffourc@etsu.edu

Sophie Dessus-Babus
East Tennessee State University

Katalin Szebeni
East Tennessee State University

Follow this and additional works at: https://dc.etsu.edu/etsu-works

Gene Expression Analyses of Neurons, Astrocytes, and Oligodendrocytes Isolated by Laser Capture Microdissection From Human Brain: Detrimental Effects of Laboratory Humidity

Copyright Statement

Gene Expression Analyses of Neurons, Astrocytes, and Oligodendrocytes Isolated by Laser Capture Microdissection From Human Brain: Detrimental Effects of Laboratory Humidity

Gregory A. Ordway[1,*], **Attila Szebeni**[1], **Michelle M. Duffourc**[1], **Sophie Dessus-Babus**[2], and **Katalin Szebeni**[1]

[1] Department of Pharmacology, James H. Quillen College of Medicine, East Tennessee State University, Johnson City, Tennessee

[2] Department of Microbiology, James H. Quillen College of Medicine, East Tennessee State University, Johnson City, Tennessee

Abstract

Laser capture microdissection (LCM) is a versatile computer-assisted dissection method that permits collection of tissue samples with a remarkable level of anatomical resolution. LCM's application to the study of human brain pathology is growing, although it is still relatively underutilized, compared with other areas of research. The present study examined factors that affect the utility of LCM, as performed with an Arcturus Veritas, in the study of gene expression in the human brain using frozen tissue sections. LCM performance was ascertained by determining cell capture efficiency and the quality of RNA extracted from human brain tissue under varying conditions. Among these, the relative humidity of the laboratory where tissue sections are stained, handled, and submitted to LCM had a profound effect on the performance of the instrument and on the quality of RNA extracted from tissue sections. Low relative humidity in the laboratory, i.e., 6–23%, was conducive to little or no degradation of RNA extracted from tissue following staining and fixation and to high capture efficiency by the LCM instrument. LCM settings were optimized as described herein to permit the selective capture of astrocytes, oligodendrocytes, and noradrenergic neurons from tissue sections containing the human locus coeruleus, as determined by the gene expression of cell-specific markers. With due regard for specific limitations, LCM can be used to evaluate the molecular pathology of individual cell types in post-mortem human brain.

Keywords

laser capture microdissection; astrocyte; oligodendrocyte; noradrenergic neuron; humidity

Laser capture microdissection (LCM) is a versatile computer-assisted dissection method that permits collection of tissue samples with a remarkable level of anatomical resolution. The method was developed at the NIH for use in studying cancer, but it has since been used in a variety of research fields. A PubMed search of the medical literature, for papers using or discussing LCM yielded 220 papers in 2007, but of these only 19 papers were found that applied LCM to study the neuropathology of human post-mortem brain tissue. This may be due in part to the difficulty in capturing individual cells from unfixed frozen tissues collected under variable conditions and at a wide range of time intervals between death and tissue collection (post-mortem interval). The appeal of LCM to researchers studying human

*Correspondence to: Gregory A. Ordway, PhD, Professor and Chair, Department of Pharmacology, James H. Quillen College of Medicine, East Tennessee State University, P.O. Box 70577, Johnson City, TN 37614. ordway@etsu.edu.

brain pathology rests prominently on the capability of LCM to permit measurement of gene expression within cells of a distinct phenotype or in a small, neuroanatomically distinct region. Many past studies of human brain biology in neurological and psychiatric disorders have utilized methods that lack this resolution; i.e., brain regions containing a variety of cellular phenotypes are typically dissected and homogenized. For cellular resolution, in situ hybridization and fluorescence immunohistochemistry have been used, but these methods have limitations such as availability of antibodies, requirement of fixed tissue, and/or difficulties with genes that have low expression levels.

A number of methodology papers have appeared regarding the uses and limitations of LCM (Mikulowska-Mennis et al., 2002; Vincent et al., 2002; Kihara et al., 2005; Kinnecom and Pachter, 2005; Bagnell, 2006; Espina et al., 2006; Kerman et al., 2006; Kube et al., 2007; Murray, 2007; Sluka et al., 2008), including a recent publication referring to the use of LCM to capture tissue from human brain specimens (Kerman et al., 2006). The present study builds on this existing literature, focusing on laboratory environment issues that affect LCM performance, particularly in its application to the dissection of frozen post-mortem human brain. Experimental conditions were tested for their effect on the efficiency of cell capture by LCM, quality of RNA isolated from captured cells, and purity or clarity of the capture of specific cell types. Although a number of instruments are available to perform LCM, the one used in the present study was the Arcturus Veritas (Molecular Devices, Sunnyvale, CA). This instrument uses the same capture technology as other Arcturus instruments, including the Arcturus Microdissection System, the Arcturus Pixcell II System, and the Arcturus AutoPix instrument. The purpose of this paper, as with other published papers on the use of LCM, is to shorten the time required for an investigator to develop the use of LCM in the capture of specific cell types from frozen human brain tissue, to increase the efficiency of use of the instrument for experienced users, and to increase the quality of captured samples. A key finding of this work is the demonstration that laboratory humidity not only reduces the performance of the LCM instrument but significantly reduces the quality of RNA in tissue sections.

MATERIALS AND METHODS

Brain Tissues

Post-mortem brain samples were obtained courtesy of Craig Stockmeier, PhD (University of Mississippi Medical Center). Brain tissues were collected at autopsy at the Cuyahoga Country Coroner's Office in Cleveland, Ohio, and informed written consent was obtained from the legal next-of-kin of all subjects in accordance with Institutional Review Board policies at Case Western Reserve University and the University of Mississippi Medical Center. Four subjects studied had no known psychiatric or neurological diseases. Subject ages ranged from 17 to 48 years (mean ± SEM 34 ± 8 years), with brain pH values ranging from 6.27 to 6.98 (mean ± SEM 6.87 ± 0.07) and post-mortem intervals ranging from 9 to 23 hr (mean ± SEM 16.9 ± 2.9 hr). Toxicology demonstrated no drugs in blood or urine except for one subject with ethanol in the blood. Subjects died from cardiovascular events (three) or homicide (one).

Tissue Preparation and Sectioning

Blocks of tissue from the pons containing locus coeruleus (LC) were frozen at autopsy and stored at −80°C. Tissue blocks were sectioned (10 μm) with a cryostat microtome (Leica CM3050 S). Attempts to use thinner sections resulted in loss of noradrenergic neurons during sectioning. Sections were mounted on a room-temperature (22°C) HistoGene LCM microslide (Molecular Devices), placed immediately in a chilled microslide box in the cryostat, and transported on ice to storage at −80°C for up to 2 months. Before sectioning

and between each tissue block, the knife holder and antiroll plate were wiped carefully with 100% ethanol to avoid cross-contamination.

Staining

For visualization of noradrenergic neurons, frozen tissue sections were stained with the HistoGene LCM Frozen Section Staining Kit (Molecular Devices) according to the manufacturer's protocol. Briefly, one or two slides were removed from the −80°C freezer and transferred into 75% ethanol (30 sec); distilled water (30 sec); LCM dye (1 min); 75%, 90%, and 100% ethanol (each for 30 sec); and xylene dehydration (5 min) and then dried in a hood for 30 sec. All slides were placed in a desiccator for 5′min until ready for LCM, except where otherwise noted. Oligodendrocytes were stained by using a modified Nissl staining protocol: cold acetone (5 min); xylene (2×1 min); 100%, 95%, and 75% ethanol (each for 30 sec); rapid dip in distilled water; cresyl violet dye (2% w/v; 2 min); rapid dip in distilled water; 75%, 95%, and 100% ethanol (each for 30 sec); and xylene (2×2 min) and then dried for 30 sec in the hood, for a total procedure time of 20 min. Astrocytes were stained with rapid glial acidic fibrillary protein (GFAP) immunocytochemistry as follows. Sections were fixed in −20°C acetone for 5 min, and endogenous peroxidase activity in the tissue was neutralized in 0.05 M TBS (pH 7.6) containing 1.5% H_2O_2 for 10 sec. After blocking with 10% normal horse serum for 10 min, sections were incubated with mouse monoclonal anti-human GFAP antibody (Chemicon, Temecula, CA; catalog No. MAB360; 1:400) for 10 min, 5 min with an appropriate secondary antibody (horse anti-mouse IgG; Vector Laboratories, Burlingame, CA; catalog No. PK-6102; 1:200), and then 5 min with avidin-biotinylated horseradish peroxidase complex. GFAP was then visualized by incubating sections in 50 ml buffer containing 0.05 M Tris, 0.3% ammonium nickel sulfate, 0.025% diaminobenzidine (pH 7.8) for 5 min, then for 5 min in another 50 ml of the same buffer but also containing 0.066% H_2O_2. Sections were given 5-sec washes in TBS (0.05 M Tris, 0.25 M NaCl, pH 7.6) between all incubation steps, except between application of serum and primary antibody. Sections were then dehydrated with the HistoGene Kit (sequential washes in 75%, 95%, and 100% ethanol, each for 30 sec). Sections were dehydrated for 5 min in xylene and then dried for 30 sec in the hood and placed in a dessicator (total time of immunostaining procedure 50 min).

LCM

LCM was performed on the Veritas Microdissection Instrument model 704 (Molecular Devices) with CapSure Macro caps (Molecular Devices). For the capture of noradrenergic neurons, surrounding tissue approximately 30–35 μm around the target cells was removed by UV laser, improving capture clarity. Optimized settings for noradrenergic cells were 60–80 mW pulse power, 2,500–2,800 μsec pulse duration, and 30–35 μm laser spot diameter. Optimized settings for astrocytes and oligodendrocytes were 40–60 mW pulse power, 1,200–1,700 μsec pulse duration, and 20–25 μm spot diameter. NE neurons were distinguished from glia cells by their larger size and neuromelanin content in the HistoGene-stained sections. Astrocytes were selected based on their GFAP staining. Oligodendrocytes, stained with Nissl, have a compact and dark nucleus, distinguishing them from the larger and more lightly stained astrocytes and smaller microglia (Hamidi et al., 2004). Oligodendrocytes selected for capture exhibited medium-sized, dark nuclei that were circular. Oligodendrocytes or oligodendrocyte-like cells with larger and lighter, round nuclei were not selected. For all cell types, cells were selected for capture using ×60 power and the naked eye to identify desired cells, rather than using the automated cell-selection procedures available on the instrument.

Relative Humidity

The effects of relative humidity on RNA quality were tested at a standard room temperature of 22°C. After staining slide-mounted tissue sections, slides were transferred to a chamber where relative humidity was adjusted to levels indicated. For 6% relative humidity, slides were placed in a desiccator under vacuum. Temperature and humidity were monitored with a hygrometer (Oregon Scientific). Slides were stored in the humidity chamber for 30, 60, 120, and 240 min. After exposures, lysis buffer was added (2×100 μl) directly onto tissue, and RNA was purified from the lysate with an RNAqueous-Micro Isolation Fit (Ambion, Austin, TX). RNA integrity (RIN) and concentration were assessed by electrophoresis using RNA Nano Chips on the Agilent 2100e Bioanalyzer running 2100 Expert Software vB.02.03 (Agilent Technologies, Waldbronn, Germany). RIN is a numerical estimate of the quality of RNA that is derived using an algorithm that takes into account the entire electrophoretic trace of the RNA sample, rather than just the 18S and 28S peaks. RIN is a robust and reliable predictor of RNA integrity (Schroeder et al., 2006).

Quantitative PCR

Total RNA was isolated from laser-captured cells using the RNAqueous Micro Kit (includes DNase treatment; Ambion). RIN values and concentrations were assessed immediately after purification by electrophoresis using RNA Nano or Pico Chips with an Agilent 2100e Bioanalyzer. RNA samples were stored at −80°C to minimize degradation. cDNA was generated from RNA using Superscript III Platinum reverse transcriptase kit (Invitrogen, Carlsbad, CA), following the manufacturer's instructions. Gene-specific primers were designed in Visual OMP (DNA Software, Inc., Ann Arbor, MI). For folding prediction of target cDNA (Zuker, 2003), Mfold web server software was used (http://www.bioinfo.rpi.edu/applications/mfold/cgi-bin/dna-forml.cgi). Primers (Table I) were designed to contain a GC content of 45–55% and to span introns to hinder amplification of genomic DNA. Quantitative end-point PCR was performed with 1 μl cDNA, 0.1 μM primers, and Eppendorf HotMasterMix Taq DNA polymerase in a final volume of 25 μl. Amplification conditions were standardized and optimized for each gene and primer set. PCR amplicons, collected during the linear range of amplification, were quantified on an Agilent 2100e Bioanalyzer using DNA 1000 Chips with a quantitative range of 0.1–50 ng/μl. PCR product yields below 0.1 ng/μl were considered below the detection limit of the assay and were therefore assigned the value of 0.

Statistical Analysis

Data were analyzed statistically by a one-way analysis of variance followed by a post-hoc test (Newman-Keuls multiple-comparisons test or Dunnett's multiple-comparisons test; GraphPad Prism 4.0; GraphPad Software, San Diego, CA) relevant for the particular experiment as described in Results. Summary statistics are reported as the mean ± SEM. $P < 0.05$ was considered significant.

RESULTS

Effect of Relative Humidity of Laboratory on LCM Performance

It was recognized early in the our use of the Arcturus Veritas that laser capture was easier to perform during the cold months of the year and that the efficiency of capture of single cells even during the winter months was a function of the amount of time for which the slide was housed in the instrument. The efficiency of capture is defined here as the number of successful captures of cells onto the CapSure cap relative to the number of cells designated for capture from the section. Given that indoor humidity is generally lower in the winter as heating systems are engaged, the effect of different relative humidities in the room where the

Veritas was housed was evaluated. This was accomplished by isolating the room from the central heating-air conditioning system, providing a separate heating-air conditioning source, and by installing dehumidifiers to control the level of humidity in the room. Three different relative humidities were tested in the LCM capture room during three different periods of time. Cells were captured from sections cut from four different post-mortem human brains at each of the three relative humidities. The same four brains were sectioned and subjected to LCM for all humidity studies. The procedure for sectioning, staining, and handling the slides was identical for each humidity, and the sectioning and staining were performed immediately (same day) prior to the LCM in each case. The room temperature was maintained at 22°C. Approximately 80% of target cells were successfully attached to the CapSure cap at relative humidities of 20% and 33%. However, capture efficiency was significantly reduced at the relative humidity of 41% (Fig. 1).

Factors Affecting RNA Quality in LCM Samples

High-quality RNA is crucial for valid quantification of gene expression. The Arcturus Veritas LCM uses a gentle infrared laser to activate film on a CapSure cap to collect tissue. Prior to initiating cell type-specific gene expression analyses, it was imperative to demonstrate that LCM does not compromise RNA quality. We compared RNA integrity, using the RIN value as the index (Imbeaud et al., 2005), in samples collected by tissue micropunch or LCM. Frontal cortex tissue samples were collected from four subjects. Samples subjected to LCM were prestained with a HistoGene LCM Frozen Section Staining Kit (20 min procedure) or a rapid GFAP immunostain (50 min procedure as described in Materials and Methods) to promote visualization of cells and to ascertain what effect, if any, the staining protocol or capture process has on the quality of isolated RNA. Total RNA was isolated from the samples using the RNAqueous (tissue punch) or RNAqueous Micro (LCM) Kits (Ambion). RNA quality was then determined with an Agilent 2100e Bioanalyzer. Neither staining procedure nor LCM significantly reduced the integrity of isolated RNA compared with that obtained from micropunched tissue samples (Fig. 2).

Given the effect of humidity in the LCM facility on capture efficiency, the possibility that exposure of tissue sections to humidity during the capture process might affect RNA quality was considered. To test this possibility, sections were collected from blocks of frozen postmortem human frontal cortex (Brodmann's area 9) from four subjects and were stained using the HistoGene LCM Frozen Section Staining Kit according to the manufacturer's directions. Stained sections were stored at different relative humidities and for several time intervals. Immediately after the exposures, sections were scraped from the slides, and RNA was isolated and subjected to quality-analysis with the Agilent Bioanalyzer. Figure 3 demonstrates that RNA quality is reduced in a time-dependent manner at a relative humidity at or above 31%.

Factors Affecting Capture Clarity

Capture clarity is defined herein as the quality of the capture of a single cell type as determined by the relative expression of cell type-specific genes. This was determined by measuring the expression levels of cell type-specific genes in multiple cell types, including in cells where gene expression should not exist or should be extremely low. To determine clarity of capture, the expression levels of the cell type-specific genes, tyrosine hydroxylase, and dopamine-β-hydroxylase (DBH; noradrenergic neuron), glial fibrillary acidic protein (astrocyte), and myelin oligodendrocyte glycoprotein (MOG; mature oligodendrocyte) were measured by using reverse transcription/quantitative end-point PCR. Reference genes selected for normalization of target gene expression were actin, ubiquitin C (UBC), and glyceraldehyde 3-phosphate dehydrogenase (GAPDH). Several factors can affect the clarity

of capture (see Discussion), but evaluated here are those easily controllable factors related to LCM instrument usage.

The Arturus Veritas LCM permits an investigator considerable flexibility in defining the physical parameters of the infrared laser that activates the CapSure film to capture cells. The manufacturer provides a well-defined method to optimize capture settings, but different settings of the laser are required depending on the size and type of cell to be captured as well as the proximity of different cell types nearby. The process of wetting refers to melting the polymer on the cap so that it fuses adequately to the tissue or cells when the laser fires. Two main features of adjustment of the laser, power and pulse, have a major influence on the wetting process and, thereby, the capture of cells. Hence, different power intensity and pulse frequency settings for capturing cells of different types from the pontine brainstem in the region of the locus coeruleus were evaluated to determine their influence on capture clarity. Using constant power settings resulted in changes in the size of the capture spot from cap to cap, from slide to slide, and even on the same slide, reducing capture clarity for all three cell types, i.e., an increase in contamination of other cell types. As shown in Figure 4, the use of constant power settings applied to the capture of oligodendrocytes resulted in marked detection of GFAP (astrocyte) and DBH (noradrenergic neuron) gene expression. In contrast, adjusting settings to restrict the spot size resulted in markedly less contamination of GFAP and DBH mRNAs.

Although adjusting the spot size to a constant size reduced contamination of surrounding cells, the usefulness of this approach does not apply equally to all cell types. Astrocytes and oligodendrocytes often have few nearby (within 20 μm) cells, and cells without nearby companions can often be found and captured from brain tissue sections. However, many neurons often have an astrocyte or oligodendrocyte in close proximity (within 5–10 μm). For example, in the locus coeruleus, neuromelanin-containing neurons often have an oligodendrocyte or astrocyte very nearby. The average diameter of a human noradrenergic neuron in the locus coeruleus is approximately 40 μm. Capturing individual noradrenergic neurons requires higher laser power settings, possibly because of the presence of neuromelanin in the neuronal cytosol that seems to interfere with the capture process. The higher power laser results in a larger spot size and increases the likelihood of capturing unwanted satellite oligodendrocytes. The unwanted neuropil and cells surrounding the neurons can be removed by using the cutting laser of the Arturas Veritas prior to capture. This method, although slow and tedious, results in extremely high capture clarity (Fig. 5A–C).

After establishment of these LCM parameters, noradrenergic neurons, astrocytes, and oligodendrocytes were captured from sections cut through the human locus coeruleus. After RNA isolation and reverse transcription, evaluation of the expression of three cell type-specific markers revealed excellent capture clarities for all three cell types, regardless of the reference gene that was used to normalize the target gene expression data (Fig. 6). In most samples, the amount of expression of a marker gene in a noncognate cell (e.g., the amount of MOG expression in sample of noradrenergic neuron) was below the detection limit of the Agilent Bioanalyzer or below 5% of the expression in the cognate cell.

Cell Number Is an Additional Factor for Normalization of Gene Expression

Noradrenergic neurons were captured from a single subject to verify whether transcript levels obtained by RT-qPCR were correlated with cell number. The Arcturas Veritas keeps a record of cells designated for capture during the process of collecting cells on the CapSure caps. However, this number must be corrected for the number of failed captures, because not all cells targeted for capture are collected. Figure 7 demonstrates linear relationships

between the number of cells collected and PCR transcript levels for actin and UBC gene expressions.

DISCUSSION

This study demonstrates several important factors that affect the LCM of frozen tissue samples, the most striking being the impact of environmental humidity on LCM. Numerous investigators have mentioned the issue of room humidity in the LCM process (Ball et al., 2002; Michel et al., 2003; Su et al., 2004; Dillon et al., 2005; Kinnecom and Pachter, 2005; Bagnell, 2006; Espina et al., 2006), suggesting that high ambient humidity lowers the efficiency of laser capture. The relative humidity for optimum performance of capture is dependent on the type of instrument that is used (Bagnell, 2006). For systems that capture the tissue by using gravity, dropping the microdissected tissue into a cap, low relative humidity results in static interference and loss of tissue. In contrast, for the Arcturus systems, Bagnell (2006) suggests that low relative humidity is required. The level of humidity recommended in the current literature varies from below 40% (Espina et al., 2006), to below 35% (Kinnecom and Pachter, 2005), to below 30% (Dillon et al., 2005). The present study empirically verified that LCM capture efficiency was best at a relative humidity at or below 33% and that this efficiency significantly deteriorated at the relative humidity of 41%. It is noteworthy that one of the first steps in tissue preparation for LCM is the sectioning of frozen tissues with a cryostat microtome. These instruments perform poorly in low humidity, because static electricity interferes with the collection of sections. The typical relative humidity in a laboratory building is 40–60%, with the American Society of Heating, Refrigerating, and Air-Conditioning Engineers (ASHRAE) recommending a maximum acceptable relative humidity of 60% at 78°F (25.5 °C; see http://www.ashrae.org/). Therefore, the optimum conditions for the entire procedure for LCM requires separate air handling environments in which temperature and humidity can be independently controlled.

Laboratory humidity also affected the quality of RNA that was extracted from tissue sections, with higher humidity resulting in increased degradation of RNA. It is not known whether this humidity-induced degradation of RNA was a result of reactivation of nascent RNAases that survived the fixation process in tissue sections or as a result of nonenzymatic hydrolysis of RNA (Kierzek, 1992). The inclusion of RNase inhibitors in the staining solution has been recommended previously to reduce RNA degradation during sample preparation (Kube et al., 2007). However, we found that this procedural inclusion did not reduce RNA degradation as a result of poststaining laboratory exposure to humidity (data not shown). Despite the mechanism of degradation, the results of this study emphasize the importance of keeping tissue sections as dry as possible following fixation, which should include keeping sections in a desiccator after staining and during transport to the LCM and maintaining relative humidity near 20% during the laser capture process. The average relatively humidity in a laboratory (40–60%) where tissue sections are stored or set following other staining and fixation methods will likely reduce RNA quality for LCM, and this may also occur for other types of RNA assays such as in situ hybridization. Some investigators state that the maximum time allowable for capture of cells by LCM is 20 (Michel et al., 2003) to 30 (Kinnecom and Pachter, 2005; Espina et al., 2006) min, because longer times result in degradation of mRNA or reduced efficiency of capture, although no specific data are provided to quantify the level of degradation. It can be inferred from the data presented here that increased degradation of RNA that occurs with time are a result of continued exposure of the slide (in the LCM apparatus) to undesirable humidity. It seems logical that the process of degradation would continue after cells have been captured on the cap and until the process of RNA isolation begins, suggesting that caps should not be left in the instrument while continuing the capture process on additional slides, unless laboratory

humidity is kept low. The present work studied the effect of LCM on RNA quality at low humidity (Fig. 2) and the effect of humidity on RNA quality prior to LCM (Fig. 3). It is possible that exposure of tissue to LCM results in an even larger effect of humidity on RNA quality, but the present research did not examine this possibility. The negative effects of humidity on LCM instrument efficiency and separately on RNA quality should sufficiently discourage researchers from performing LCM under conditions other than low relative humidity.

The Arcturus Veritas has an enclosed environment for sample dissection, which "minimizes potential for sample contamination, as well as the impact of other environmental variables, such as temperature, humidity and ambient light" (see http://www.moleculardevices.com/pages/instruments/veritas_md_track.html). However, we are not aware of any mechanism within the main assembly of the instrument that controls humidity, so it can be presumed that the humidity inside the instrument is very similar to the environment outside the instrument. Nevertheless, slides are contained inside the instrument away from humidity from the experimenter's exhaled air, which could potentially contribute to degradation of RNA compared with an instrument without this added protection, although this in only speculation, insofar as we have not specifically studied the effect of exhaled air on RNA degradation.

Although many of the publications describing LCM methodology state that a dehumidifier was placed in the room housing the LCM, we were unable to find a manuscript that reported the systematic monitoring of the humidity in the room during the LCM. To reach a humidity of 23% in our LCM facility to permit optimal LCM conditions during the warmer months of the year, it was necessary to install a separate air-handling system, including three dehumidifiers, one standard room dehumidifier, one commercial dehumidifier, and a dehumidifying stand-alone air conditioning unit. When humidity in the room that houses the LCM was maintained at 23% or below, the time permissible for efficient capture of cells with negligible RNA degradation was increased considerably, permitting capture of cells from a single slide for 2 hr without measurable RNA degradation. This increase in time for capture greatly increases the speed at which LCM can be performed (more cells can be collected from a single slide) and decreases the cost of LCM because fewer CapSure caps, fewer slides, and less of the reagents are required to obtain an adequate amount of tissue.

When using LCM to capture cells to compare gene expression between two groups of subjects, it may at first seem that good scientific method would require that the power settings of the laser should be held constant for all tissue sections. However, maintaining laser settings constant for specific cell types resulted in lower clarity of capture, i.e., the capture of unwanted surrounding cells. Capture clarity was best when power settings were adjusted to maintain a predefined diameter of the laser spot size. For certain cell types, simply adjusting the laser spot size is insufficient to ensure capture clarity. For example, in the capture of noradrenergic neurons of the locus coeruleus, it was necessary to use the ultraviolet laser to burn neuropil and surrounding cell bodies because of the high frequency at which oligodendrocytes were found in very close proximity (<10 μm). In contrast, the capture of astrocytes and oligodendrocytes did not require this additional step.

The selection of appropriate reference genes to normalize gene expression data has been discussed and reviewed in several recent publications (Vandesompele et al., 2002; Radonic et al., 2004; Bustin et al., 2005). During LCM, the numbers of cells that are captured onto the cap can be easily counted, so cell number can be used to check the normalization of data or used as a reference itself. However, some caveats for the use of cell number should be considered. First, as mentioned in Results, the Acrturas Veritas counts the number of cells that are marked for capture, but it does not record the number of successful captures. This

requires the investigator to keep track of the number of failures so that the target count can be corrected. Also, sometimes only a part of a cell is captured, rather than the whole cell. This was particularly an issue for large cells such as locus coeruleus neurons. In addition, cell size varies, as does the amount of a particular cell that occurs in a 10-μm-thick tissue section. That is, it is possible that only a fraction of the entire cell occurs within the tissue section. These issues, along with the possibility of variable efficiencies of RNA extraction and reverse transcription between samples, demonstrate the importance of the use of traditional references (i.e., reference gene expressions) other than cell number to normalize data. Despite these potential problems, the present study demonstrated a strong correlation between captured cell number and gene expression levels, indicating that cell number is a useful reference check for gene expression normalization.

In summary, the effect of environmental humidity on RNA quality in the context of specific methods designed to evaluate RNA in tissue sections requires careful consideration. The present study demonstrates that, with relative humidity maintained at or below 23%, the process of laser microdissection operated at high efficiency of capture and did not reduce the quality of RNA for a collection period up to 2 hr. Under these conditions, LCM was used successfully to capture selectively astrocytes, oligodendrocytes, and locus coeruleus neurons and to measure their gene expression. By using cell type-specific gene expression to evaluate the clarity of capture, contamination of noncell type-specific mRNAs was undetectable. Analysis of clarity with gene expression markers for desired and undesired cells permits the evaluation of each sample prior to performing quantitative analyses of gene expression levels in specific cell types. An upper limit of acceptable contamination of gene expression from other cell types (e.g., 5%) can be set a priori so that, if a particular sample demonstrates a greater than acceptable expression of a marker gene, a researcher can dispose of the sample and perform another LCM of sections cut from the same tissue block. When combined with quantitative RT-PCR methods, LCM is a powerful tool for evaluating the gene expression of specific cell types in the human brain, and its use provides investigators with the opportunity to advance our understanding of the molecular pathology of brain diseases.

Acknowledgments

References

Bagnell, CR. Laser capture microdissection. In: Coleman, WB.; Tsongalis, GJ., editors. Molecular diagnostics: for the clinical laboratorian. 2. Totowa, NJ: Humana Press Inc; 2006. p. 219-224.

Ball HJ, McParland B, Driussi C, Hunt NH. Isolating vessels from the mouse brain for gene expression analysis using laser capture microdissection. Brain Res Brain Res Protoc. 2002; 9:206–213. [PubMed: 12113780]

Bustin SA, Benes V, Nolan T, Pfaffl MW. Quantitative real-time RT-PCR—a perspective. J Mol Endocrinol. 2005; 34:597–601. [PubMed: 15956331]

Dillon D, Zheng K, Negin B, Costa J. Detection of Ki-ras and p53 mutations by laser capture microdissection/PCR/SSCP. Methods Mol Biol. 2005; 293:57–67. [PubMed: 16028410]

Espina V, Wulfkuhle JD, Calvert VS, VanMeter A, Zhou W, Coukos G, Geho DH, Petricoin EF 3rd, Liotta LA. Laser-capture microdissection. Nat Protoc. 2006; 1:586–603. [PubMed: 17406286]

Hamidi M, Drevets WC, Price JL. Glial reduction in amygdala in major depressive disorder is due to oligodendrocytes. Biol Psychiatry. 2004; 55:563–569. [PubMed: 15013824]

Imbeaud S, Graudens E, Boulanger V, Barlet X, Zaborski P, Eveno E, Mueller O, Schroeder A, Auffray C. Towards standardization of RNA quality assessment using user-independent classifiers of microcapillary electrophoresis traces. Nucleic Acids Res. 2005; 33:e56. [PubMed: 15800207]

Kerman IA, Buck BJ, Evans SJ, Akil H, Watson SJ. Combining laser capture microdissection with quantitative real-time PCR: effects of tissue manipulation on RNA quality and gene expression. J Neurosci Methods. 2006; 153:71–85. [PubMed: 16337273]

Kierzek R. Nonenzymatic hydrolysis of oligoribonucleotides. Nucleic Acids Res. 1992; 20:5079–5084. [PubMed: 1408824]

Kihara AH, Moriscot AS, Ferreira PJ, Hamassaki DE. Protecting RNA in fixed tissue: an alternative method for LCM users. J Neurosci Methods. 2005; 148:103–107. [PubMed: 16026852]

Kinnecom K, Pachter JS. Selective capture of endothelial and perivascular cells from brain microvessels using laser capture microdissection. Brain Res Brain Res Protoc. 2005; 16:1–9. [PubMed: 16168706]

Kube DM, Savci-Heijink CD, Lamblin AF, Kosari F, Vasmatzis G, Cheville JC, Connelly DP, Klee GG. Optimization of laser capture microdissection and RNA amplification for gene expression profiling of prostate cancer. BMC Mol Biol [electronic resource]. 2007; 8:25.

Michel C, Desdouets C, Sacre-Salem B, Gautier JC, Roberts R, Boitier E. Liver gene expression profiles of rats treated with clofibric acid: comparison of whole liver and laser capture microdissected liver. Am J Pathol. 2003; 163:2191–2199. [PubMed: 14633594]

Mikulowska-Mennis A, Taylor TB, Vishnu P, Michie SA, Raja R, Horner N, Kunitake ST. High-quality RNA from cells isolated by laser capture microdissection. Biotechniques. 2002; 33:176–179. [PubMed: 12139243]

Murray GI. An overview of laser microdissection technologies. Acta Histochem. 2007; 109:171–176. [PubMed: 17462720]

Radonic A, Thulke S, Mackay IM, Landt O, Siegert W, Nitsche A. Guideline to reference gene selection for quantitative real-time PCR. Biochem Biophys Res Commun. 2004; 313:856–862. [PubMed: 14706621]

Schroeder A, Mueller O, Stocker S, Salowsky R, Leiber M, Gassmann M, Lightfoot S, Menzel W, Granzow M, Ragg T. The RIN: an RNA integrity number for assigning integrity values to RNA measurements. BMC Mol Biol [electronic resource]. 2006; 7:3.

Sluka P, O'Donnell L, McLachlan RI, Stanton PG. Application of laser-capture microdissection to analysis of gene expression in the testis. Prog Histochem Cytochem. 2008; 42:173–201. [PubMed: 18243898]

Su JM, Perlaky L, Li XN, Leung HC, Antalffy B, Armstrong D, Lau CC. Comparison of ethanol versus formalin fixation on preservation of histology and RNA in laser capture microdissected brain tissues. Brain Pathol. 2004; 14:175–182. [PubMed: 15193030]

Vandesompele J, De Preter K, Pattyn F, Poppe B, Van Roy N, De Paepe A, Speleman F. Accurate normalization of real-time quantitative RT-PCR data by geometric averaging of multiple internal control genes. Genome Biol. 2002; 3:RESEARCH0034. [PubMed: 12184808]

Vincent VA, DeVoss JJ, Ryan HS, Murphy GM Jr. Analysis of neuronal gene expression with laser capture microdissection. J Neurosci Res. 2002; 69:578–586. [PubMed: 12210823]

Zuker M. Mfold web server for nucleic acid folding and hybridization prediction. Nucleic Acids Res. 2003; 31:3406–3415. [PubMed: 12824337]
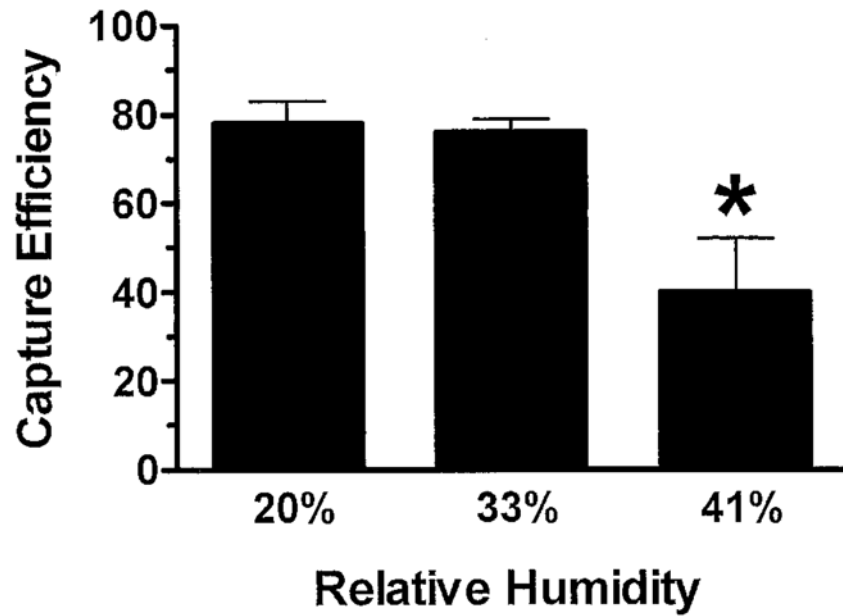
Fig. 1.
Effect of relative humidity on the efficiency of capture of cells by LCM. Shown are the mean ± SEM of percentage efficiency of capture of targeted cells computed from brainstem tissue collected from four human subjects. The asterisk indicates statistical significance comparing the 41% relative humidity group with each of the other two groups (Neuman-Keuls multiple-comparisons test; $P < 0.05$).
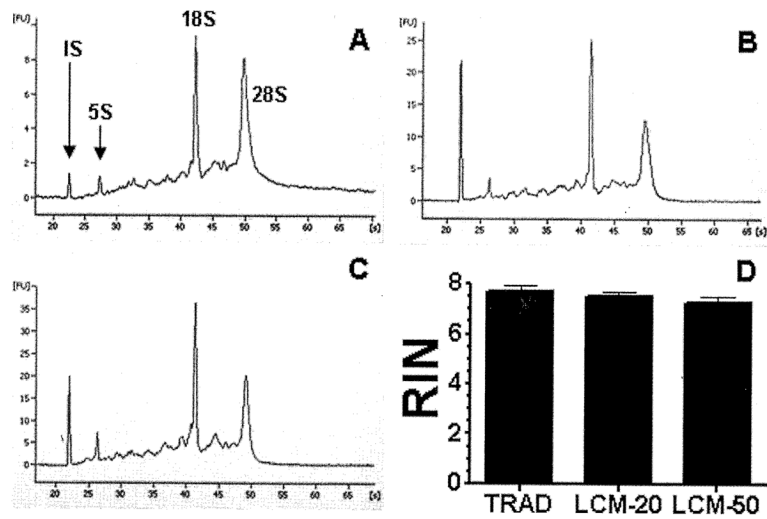
Fig. 2.
Assessment of human cerebellar RNA quality after traditional tissue extraction (**A**) and after collection of tissue by laser capture using 20 (**B**) or 50 (**C**) min tissue staining methods. Shown are representative Agilent electropherograms for each condition from a single subject (IS internal standard location; 5S, 18S, 28S rRNAs noted by arrows). **D** shows average RIN values (±SEM; n = 4 subjects) obtained from traditional tissue extraction (TRAD) and from RNA isolations of LCM samples using 20 (LCM-20) and 50 (LCM-50) min staining methods. The handling of sections and capture by LCM occurred over a 2-hr period at 20% relative humidity.
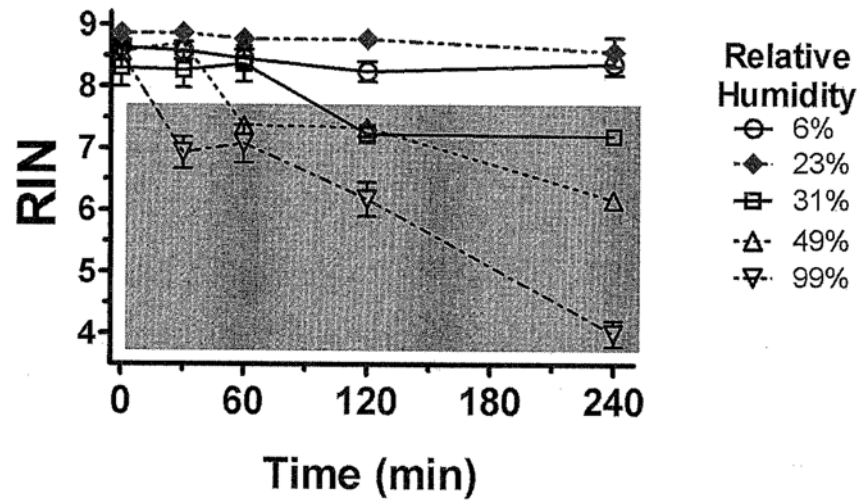
Fig. 3.
Effect of exposure of stained, slide-mounted brain tissue sections to different relative humidities on RNA quality (RIN). Sections were cut from three or four subjects, and data are presented as the mean ± SEM. All data points lying within the shaded area were significantly lower than their respective 0 time point (Dunnett's multiple-comparisons test; $P < 0.05$). Error bars are smaller than the symbol for some data points.
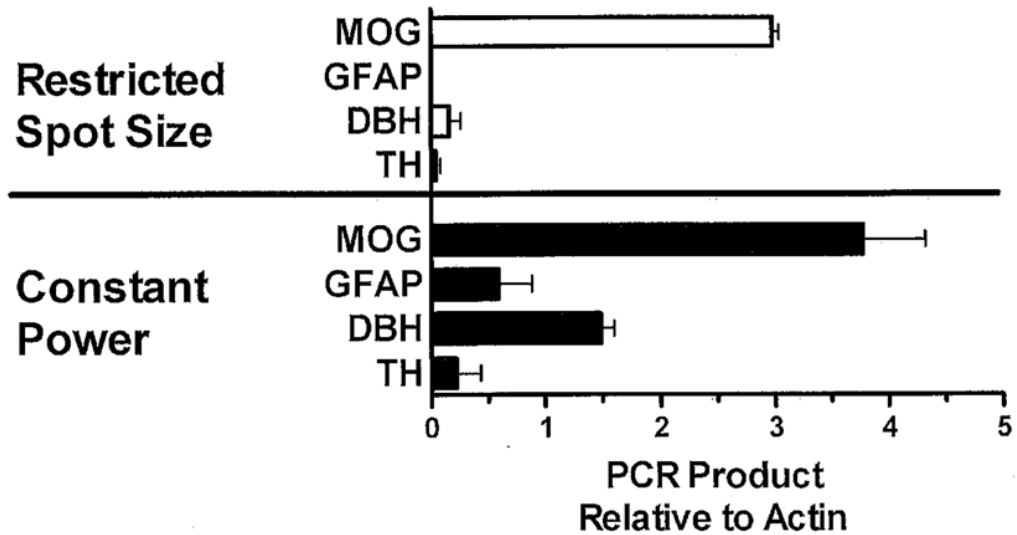
Fig. 4.
Effect of adjusting pulse and power settings to optimize capture clarity of oligodendrocytes from post-mortem human pontine tissue sections. After adjusting LCM settings to optimize oligodendrocyte capture with the first few cells, keeping those settings constant (power 40 mW, pulse 2,800 μsec, delay 100 msec, number of hits 2) yielded contamination of oligodendrocyte mRNA with mRNAs from surrounding astrocytes (GFAP) and norepinephrine neurons (DBH and TH). In contrast, repeatedly manipulating power and pulse settings to restrict the size of the capture spot yielded less contamination of mRNAs from other cell types. Shown are data from four subjects. Normalization to other reference genes (UBC and GAPDH) produced nearly identical results. Relative humidity during cell capture was 20%. Changes in power and pulse settings to maintain spot size were in a range that did not affect capture efficiency.
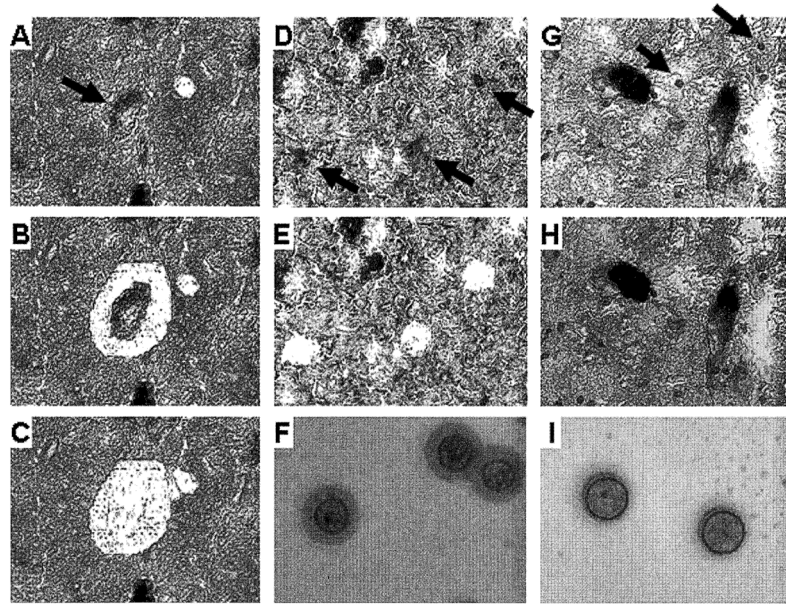
Fig. 5.
LCM of neuromelanin-containing neurons (**A–C**), GFAP-labeled astrocytes (**D–F**), and Nisslstained oligodendrocytes (**G–I**). Arrows point to cells targeted for capture (top panels; A,D,G). Large dark spots are neuromelanin-containing (noradrenergic) neurons. For noradrenergic neurons, immediately adjacent tissue was removed using the UV laser (B). C, E, and H show the tissue section after cell capture. F and I show astrocytes and oligodendrocytes, respectively, captured on the CapSure film.
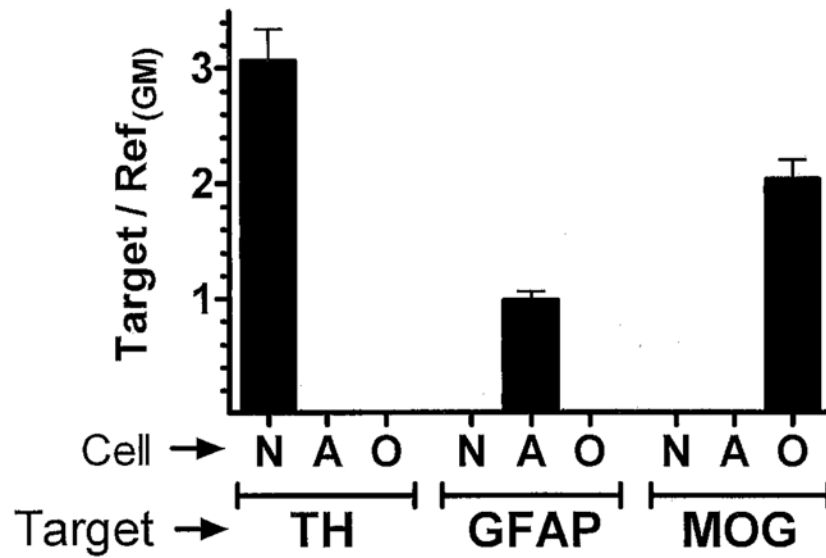
Fig. 6.
Relative expression levels of three cell type-specific genes in noradrenergic neurons (N), astrocytes (A), and oligodendrocytes (○) collected from sections cut through the human locus coeruleus. Target genes were normalized to the geometric mean of three different reference genes (GAPDH, actin, and UBC). Shown are the means ± SEM of measurements from four subjects. Levels of gene expression were below detection limits for bars not shown.
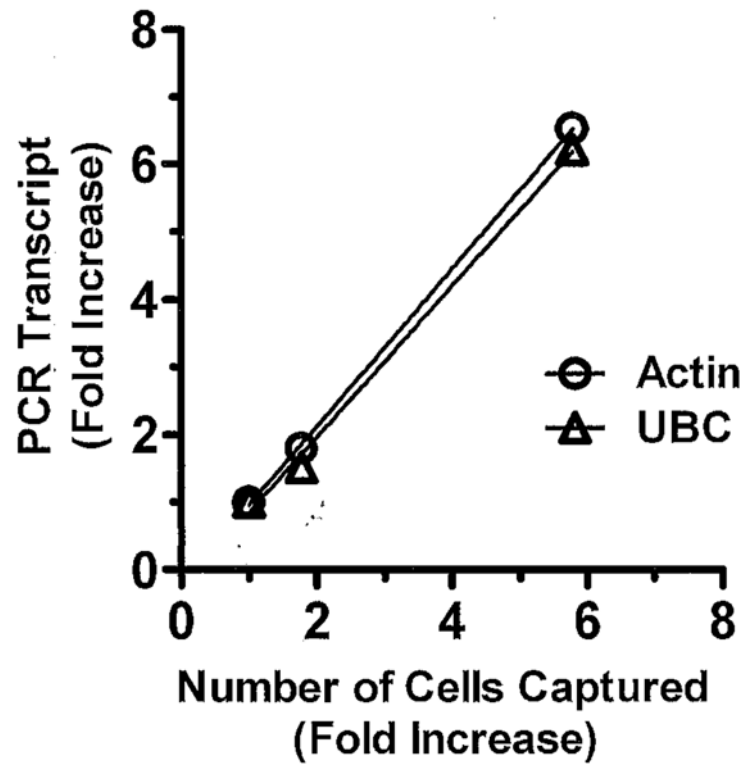
Fig. 7.
PCR amplification of actin and UBC cDNAs reversed transcribed from RNA isolated from human noradrenergic neurons. Neurons were captured by LCM from sections cut through the human locus coeruleus. Captured neurons ranged from 54 cells (onefold) to 312 cells (nearly sixfold).

Table I

Primer Sequences of Target and Reference Genes

Target or reference	Genbank No.	Primer sequence	PCR product size (bp)
β-Actin	NM_001101	(f) 5′-GCACCCAGCACAATGAAGATCAAG	128
		(r) 5′-TCATACTCCTGCTTGCTGATCCAC	
GAPDH	NM_002046	(f) 5′-TGCACCACCAACTGCTTAGC	87
		(r) 5′-GGCATGGACTGTGGTCATGAG	
GFAP	NM_002055	(f) ′-AAGCTGCTAGAGGGCGAGGAGAAC	99
		(r) 5′-TGACACAGACTTGGTGTCCAGGCT	
MOG	NM_002433.3	(f) 5′-CCTGCTGGAAGATAACCCTGTTTG	134
	NM_206809.2	(r) 5′-CACTCAGAAGGGATTTCGTAGCTC	
TH	NM_199292	(f) 5′-TCCACGCTGTACTGGTTCACGG	123
	NM_199293.2	(r) 5′-AGGCTCCTCAGACAGGCAGTG	
	NM_000360.3	(f) 5′-ATTTGGGTCGCGGTTCTTG	
UBC	NM_021009	(r) 5′-TGCCTTGACATTCTCGATGGT	133